Mol Neurobiol (2010) 41:149–158
DOI 10.1007/s12035-010-8112-x

Arginine Metabolising Enzymes as Therapeutic Tools for Alzheimer's Disease: Peptidyl Arginine Deiminase Catalyses Fibrillogenesis of β-amyloid Peptides

Peter Mohlake · Chris G. Whiteley

Received: 11 December 2009 / Accepted: 18 February 2010 / Published online: 12 March 2010

Abstract The accumulation of arginine in the cerebrospinal fluid and brains of patients suffering from acute neurodegenerative diseases like Alzheimer's disease, point to defects in the metabolic pathways involving this amino acids. The deposits of neurofibrillary tangles and senile plaques perhaps as a consequence of fibrillogenesis of β-amyloid peptides has also been shown to be a hallmark in the aetiology of certain neurodegenerative diseases. Peptidylarginine deiminase (PAD II) is an enzyme that uses arginine as a substrate and we now show that PAD II not only binds with the peptides $A\beta_{1\text{-}40}$, $A\beta_{22\text{-}35}$, $A\beta_{17\text{-}28}$, $A\beta_{25\text{-}35}$ and $A\beta_{32\text{-}35}$ but assists in the proteolytic degradation of these peptides with the concomitant formation of insoluble fibrils. PAD was purified in 12.5% yield and 137 fold with a specific activity of 59 μmol $min^{-1} mg^{-1}$ from bovine brain by chromatography on diethylaminoethyl (DEAE)-Sephacel. Characterisation of the enzyme gave a pH and temperature optima of 7.5°C and 68°C, respectively, and the enzyme lost 50% activity within 38 min at this temperature. Michaelis-Menten kinetics established a V_{max} and K_m of 1.57 μmol $min^{-1} ml^{-1}$ and 1.35 mM, respectively, with N-benzoyl arginine ethyl ester as substrate. Kinetic analysis was used to measure the affinity (K_i) of the amyloid peptides to PAD with values between 1.4 and 4.6 μM. The formation of Aβ fibrils was rate limiting involving an initial lag time of about 24 h that was dependent on the concentration of the amyloid peptides. Turbidity measurements at 400 nm, Congo Red assay and Thioflavin-T staining fluorescence were used to establish the aggregation kinetics of PAD-induced fibril formation.

Keywords Peptidyl arginine deiminase · Alzheimer disease · Amyloid peptides · Fibrillogenesis

P. Mohlake · C. G. Whiteley (✉)
Department of Biochemistry, Microbiology and Biotechnology, Rhodes University,
P.O. Box 94, Grahamstown 6140, South Africa
e-mail: C.Whiteley@ru.ac.za

Introduction

There appears little doubt, from reports in the recent literature [1, 2], that the deposition of neurofibrillary tangles and aggregated β-amyloid senile plaques in the human brain can be characterised as a hallmark in the neuropathology of Alzheimer's disease [3]. An understanding of the mechanism of their formation remains elusive and discovering drugs and/or metabolites that can inhibit the progression of the neurological disorder requires an understanding of the molecular causes underlying the neurodegenerative processes. The cerebrospinal fluid analysis of Alzheimer's patients has elevated levels of arginine though it remains uncertain whether this is a cause or is as a result of the disorder. Consequently, it follows that a therapeutic tool in the aetiology and pathogenesis of Alzheimer's disease may be to investigate arginine-metabolising enzymes and their intimate association with amyloid peptides. Peptidylarginine deiminase (PAD II) [EC.3.5.3.15] is a post-translationally modified enzyme that uses protein-arginine as a substrate producing protein-citrulline and ammonia as products (Fig. 1). This reaction, localised within the astrocytes in the brain, induces proteins in the cellular environment to unfold and trigger the aggregation of susceptible peptides [4] such as amyloid peptides. An understanding of the function and action of PAD, with respect to amyloid peptide aggregation and subsequent formation of senile plaques, may facilitate an understanding of neurodegeneration in Alzheimer's disease.

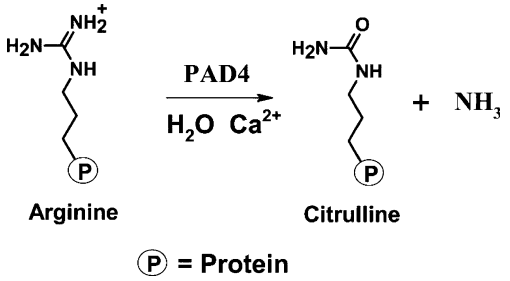

Fig. 1 Schematic representation of enzyme reaction for protein (peptidyl) arginine deiminase

A previous communication from our group [5] reported that certain amyloid peptide fragments appeared to inhibit PAD but no conclusions were made on the exact interaction of the binding and the sequence of amino acid residues responsible.

Insoluble amyloid plaques are surrounded by astrocytes which also function to store arginine reserves in brain tissue. There is, therefore, a potential connection between amyloid formation and brain arginine concentration. Little is known of the removal of amyloid peptides in vivo and it is thought that a decrease in Aβ catabolism is directly responsible for the accumulation of this peptide in the brain and its subsequent aggregation and plaque formation [6]. The higher the concentration of Aβ in vivo, the more likely they are to aggregate and form insoluble plaques. Amyloid fibrils are generally formed through a process of assembly of amyloid proteins either self-induced or by a proteolytic mechanism. It is relatively well-known [4–6] that there are a number of amyloidogenic proteins and short peptide fragments, including β-peptide itself and the neurotoxic $A\beta_{25\text{-}35}$ fragment that are capable of producing amyloid fibrils [7–9]

This present study uses a series of readily available different-sized Aβ peptides [$A\beta_{17\text{-}28}$, $A\beta_{22\text{-}35}$ and $A\beta_{32\text{-}35}$] along with the neurotoxic element $A\beta_{25\text{-}35}$ and $A\beta_{1\text{-}40}$, which is the major component of the amyloid deposits, in order to investigate which sequence would, primarily, be involved in the formation of amyloid fibrils by PAD. Kinetic analysis was used to measure the kinetic parameters (V_{max}, K_m) and affinity constants (K_i) while turbidity at 400 nm, Congo Red assay and Thioflavin-T staining fluorescence were used to establish the formation of insoluble fibrils and aggregation kinetics of PAD-induced fibril formation.

Methodology

Materials

Coomasie Brilliant Blue R-250 Stain, Sephacryl S-200, DEAE-Sephacel, amyloid peptides $A\beta_{1\text{-}40}$, $A\beta_{22\text{-}35}$, $A\beta_{17\text{-}28}$, $A\beta_{25\text{-}35}$ and $A\beta_{32\text{-}35}$, bovine serum albumen, N-benzoyl arginine ethyl ester (BAEE), bromophenol blue, ethylenediaminetetraacetic acid (EDTA), phenylmethylsulphonylfluorides (PMSF), dithiothreitol (DTT), 4-(2-hydroxyethyl) piperazine-N'-(2-ethane-sulphonic acid monosodium salt (HEPES), Tris, arginine, were obtained from Sigma-Aldrich (South Africa). A standard molecular weight marker peq-GOLD 10-170 kDa was obtained from Optima Scientific (South Africa). UV analyses were carried out on a PowerWave microplate spectrophotometer (Bio-Tek Instruments) with 96-well plates, operated at 1 nm bandwidth using the KC Junior software programme. Fluorescence analysis was carried out using a Hitachi F-2500 spectrofluorimeter.

Isolation and Purification of PAD

Bovine brain (200 g), collected fresh from a local abattoir, was homogenised in HEPES buffer (50 mM, pH7.6, 600 ml) that contained EDTA (1.0 mM), DTT (0.5 mM) and PMSF (0.43 mM) and stored as 20 ml aliquots at −70°C until required. Crude brain extract (20 ml) was sonicated (10 W, 30 s intervals, 4 min) followed by centrifugation (10,000×*g*, 4°C, 30 min) and the cell free supernatant extract, assayed for PAD activity and protein and then used for further analyses.

This sample (2 ml) was applied onto a Sephacryl S-200 column (1.5×17 cm) pre-washed with buffer Tris-HCl buffer (pH7.6, 50 mM) containing PMSF (0.43 mM) and DTT (0.5 mM) and equilibrated until A_{280} of the eluate had reached baseline. The sample was eluted in the same buffer at a flow rate of 2 ml min^{-1} and fractions (4 ml) collected, assayed for PAD and protein and active fractions pooled and dialysed overnight against Tris-HCl buffer (pH7.6, 10 mM). This cell free extract (15 ml) was then placed in a beaker, covered completely with a dry matrix of PEG 20000 and left to stand (4°C, 3 h) until the desired volume (2 ml) was obtained.

Following a similar chromatographic procedure, the cell-free supernatant brain extract (2 ml) was applied onto a DEAE-Sephacel column (1.5×17 cm) pre-washed with exactly the same buffer as before containing PMSF and DTT and equilibrated until A_{280} of the eluate had reached baseline. The sample was again eluted with the same buffer at a flow rate of 2 ml min^{-1} and fractions (4 ml) collected. These were assayed for PAD and protein and active fractions pooled, dialysed overnight against Tris-HCl buffer (pH7.6, 10 mM) and finally concentrated using PEG-20000

Statistical Analyses

All analyses were carried in triplicate and values reported as the means with standard deviation. $P<0.05$ versus control.

Where necessary analysis of variance was conducted using Statistica (data analysis software) for Windows, Version 8 (StatSoft Inc.) and Microsoft Excel 2007

Assay of PAD

PAD activity was determined by a slight modification to that previously reported [10]. The rate of ammonia production was determined spectrophotometrically by measuring the decrease in NADH absorbance at 340 nm in a coupled reaction using glutamate dehydrogenase (GDH). The standard reaction mixture for the assay contained NADH (10 mM), α-ketoglutarate (200 μM), $CaCl_2$ (10 mM), BAEE (4 mM), DTT (2.5 mM), Triton X-100 (1%), GDH (2U) in Tris HCL (pH7.5, 100 mM) in a final volume of 280 μl. The reaction was initiated by the addition of 20 μL of an appropriately diluted PAD solution. One unit of activity is the amount of enzyme that catalyses the decrease of 1 μmol of NADH per min (ε_{NADH}=6.22 $mM^{-1}cm^{-1}$)

Protein Determination

Protein was quantified by the Bradford method [11], using bovine serum albumin as a standard.

Characterization of PAD

pH, Temperature, Stability and Kinetic Profiles

The temperature optimum of the partially purified enzyme was determined in Tris-HCl buffer (pH7.5, 50 mM) over a range of 20-80°C. The reaction was started by addition of enzyme suspension (100 μl) at the different temperatures.

The optimum pH for the PAD was established by re-suspending the partially purified enzyme (100 μl) in different pH buffers (3 ml), sodium acetate (pH3.5-5.5, 50 mM); HEPES buffer (pH6-7, 50 mM) and Tris-HCI buffer (pH7.5-9, 50 mM). The PAD activity was determined in each of the samples at the different pH levels. It should be noted that, in view of the relatively short half-life of the enzyme at the established optimal temperature of 68°C, the optimum pH was determined at 50°C.

The optimum pH and temperature were used to determine the optimal thermal stability of the enzyme. PAD activity at time zero was considered to be 100% relative activity, and its activity measured at 10-min intervals for 60 min.

The kinetic properties (K_m and V_{max}) were determined by varying the substrate (benzoyl arginine ethyl ester, 300 μl) concentration between the ranges 0-4 mM. PAD activity was determined at each substrate concentration.

SDS-PAGE Analysis and Molecular Mass Determinations

The effectiveness of the purification process was determined by sodium dodecyl sulphate polyacrylamide gel electrophoresis (SDS-PAGE) on samples exhibiting deiminase activity. Samples from each purification step (20 μl) and a standard molecular weight marker (10-170 kDa), were electrophoresed on 15% SDS-PAGE at 120 V. The gels were stained with Coomassie Brilliant Blue R-250, then destained in methanol/acetic acid/water (1:1:8 *v/v/v*). The molecular weight of the partially purified PAD was determined using a standard curve of log molecular weight versus distance migrated.

Affinity of Amyloid Peptides with PAD

Kinetic Analysis

Partially purified PAD (100 μl) in Tris HCl buffer (100 mM, pH7.6) was treated with amyloid peptides $A\beta_{1\text{-}40}$, $A\beta_{22\text{-}35}$, $A\beta_{17\text{-}28}$, $A\beta_{25\text{-}35}$ and $A\beta_{32\text{-}35}$ at varying concentrations up to 30 μM in a total volume of 300 μl and in the presence of substrate (BAEE) at concentrations (0–4 mM). Enzyme activity was determined at each level of substrate concentration.

Congo Red Assay

Partially purified PAD (100 μl) in Tris HCl buffer (100 mM, pH7.6) was incubated with amyloid peptides $A\beta_{1\text{-}40}$, $A\beta_{22\text{-}35}$, $A\beta_{17\text{-}28}$, $A\beta_{25\text{-}35}$ and $A\beta_{32\text{-}35}$ at varying concentrations up to 30 μM in a total volume of 300 μl. At periodic intervals over several days, aliquots (40 μl) were incubated (30 min) with Congo Red (25 μM) in Tris-HCl buffer (pH7.6, 100 mM) containing NaCl (150 mM) in a final volume of 1.0 ml. Absorbance was read at 480 and 540 nm and the degree of fibrillogenesis estimated from the amount of Congo Red bound to the fibrils (Eq. 1) where the values 25.955 and 46.306 are the extinction coefficients of Congo Red-fibril complex and Congo Red, in units of ml μmol^{-1} respectively [12].

$$\text{Bound Congo Red}(\mu M) = \left[A^{540}/25.955\right] - \left[A^{480}/46.306\right] \quad (1)$$

Thioflavin-T Assay

Thioflavin-T (Th-T) was used to indicate the presence of AB fibrils using a modified version of that previously reported [13–15]. PAD solution (5 μl) was added to a reaction mixture containing Th-T (2 μl, 3.14 mM) and NaOH (200 μl, 10 mM) in Tris HCl buffer (pH7.6,

100 mM) and NaCl (150 mM) in a final volume of 1.0 ml. Increasing concentrations of Aβ peptides were added, incubated for 10 min at room temperature and the shift in fluorescence monitored at excitation wavelength of 440 nm and emission wavelength of 480 nm.

Turbidity Assay

Partially purified PAD (100 μl) in Tris HCl buffer (100 mM, pH7.6) was incubated with amyloid peptides $A\beta_{1\text{-}40}$, $A\beta_{22\text{-}35}$, $A\beta_{17\text{-}28}$, $A\beta_{25\text{-}35}$ and $A\beta_{32\text{-}35}$ at varying concentrations up to 30 μM in a total volume of 300 μl. Aggregation was measured by turbidity at 400 nm.

Transmission Electron Microscopy

A 10-μl sample of either amyloid peptide alone or those that had been challenged with PAD was placed onto a carbon-coated copper grid, excess liquid removed by carefully blotting with filter paper and then the sample negatively stained with uranyl acetate (2%, 30 s), washed twice in deionised water, blotted dry with filter paper and viewed using a JEOL 120C *X*2 transmission electron microscopy at acceleration voltage of 80 kV.

Results and Discussion

Isolation and Purification of PAD

A summary of the purification protocol of PAD after Sephacryl S-200 and DEAE-Sephacel chromatography is shown (Table 1).

The crude brain extract was loaded onto a Sephacryl S-200 chromatography column and the sample eluted with Tris.HCl buffer (50 mM, pH7.6). The elution profile indicated two main protein peak areas (Fig. 2a), peak 1 (fractions 3-9) and peak 2 (fractions 9–14) with only the latter peak containing PAD activity. The specific activity of this fraction was 33.1 μmol $min^{-1} mg^{-1}$ and the overall fold purification was 77 with 12.2% recovery. A similar chromatography protocol was observed after the crude enzyme was subjected to a chromatographic protocol on a DEAE-Sephacel column and eluted with the same buffer

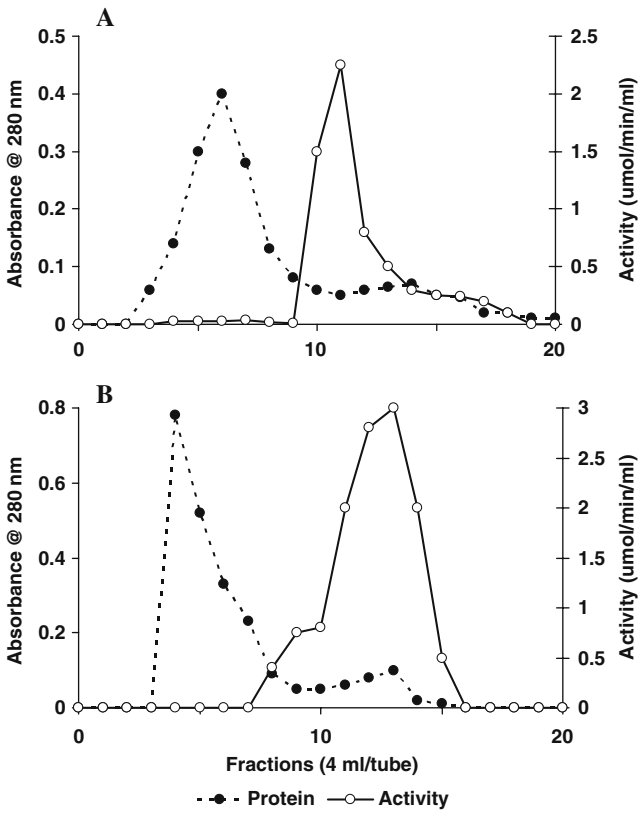

Fig. 2 Size exclusion-ion exchange chromatography of PAD. **a** Sephacryl S-200; **b** DEAE-Sephacel. Column dimension (1.5× 17 cm); flow rate: 2 ml min^{-1}. The PAD activity was eluted with Tris-HCl buffer (pH7.6, 50 mM)

(Fig. 2b). Two main protein peak areas were seen—peak 1 (fractions 3-8) and peak 2 (fractions 10–16) with only the latter containing PAD activity. The specific activity of this fraction was 59 μmol $min^{-1} mg^{-1}$ and the overall fold purification was 137 with 12.5% recovery.

SDS-PAGE analysis revealed a molecular mass of about 75,000 (data not shown) and, based upon reports from literature, we confirmed that the enzyme was homodimeric.

Characterisation of PAD

Temperature, pH and Thermal Stability

The PAD purified in this study had temperature and pH optima of 68°C and 7.5, respectively (Figs. 3a and 3b). At

Table 1 Purification table for PAD

Purification step	Total protein (mg)	Total activity (μmol/min)	Specific activity (μmol/min/mg)	Recovery %	Purification fold
Crude	195.0	84.7	0.43	100	1
Sephacryl 200	0.31	10.32	33.1	12.2	77
DEAE Sephacel	0.18	10.62	59.0	12.5	137

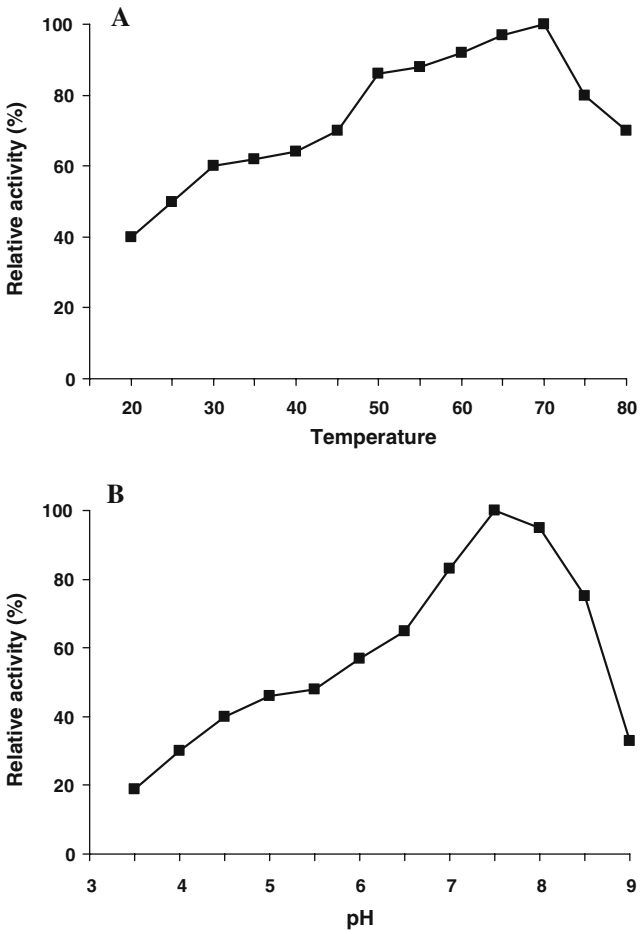

Fig. 3 **a** Temperature; **b** pH profile of the purified PAD enzyme. 100%=1.6 μmol $min^{-1}ml^{-1}$. All analyses were carried in triplicate and values reported as the means with standard deviation

pH8.5, there was 74% activity remaining that decreased substantially to 30% at pH9 while at pH6.5 there was only 60% activity decreasing to 40% at pH4.5. These values were well within those reported in the literature with optimum pH ranging between pH9 [16] and pH7 [17] with an activity of between 50% and 75% within 2 pH units of these optimal values.

The optimal temperature was considered to be quite high at 68°C with only 30% activity being lost at both 45°C and 80°C indicating a thermally stable enzyme. Reports in the literature have also indicated that PAD has optimal temperatures from 55-60°C with activity still remaining 20°C either side of this maximum [18–20].

The thermal stability of the purified PAD was investigated at optimum pH and at 25°C, 37°C and optimum temperature. There was no observable decrease in activity over 60 min when the enzyme was held at either 25 or 37°C (Fig. 4). At optimum temperature, however, minimal activity loss was observed during the initial 10 min, but thereafter, activity steadily decreased as incubation time

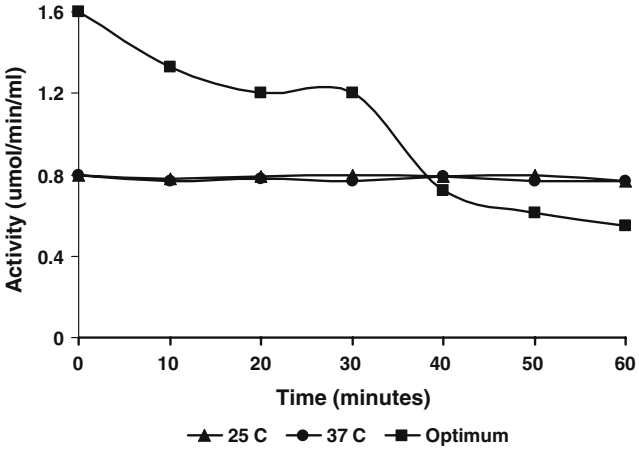

Fig. 4 Thermal stability of PAD at 25, 37 and 68°C. All analyses were carried in triplicate and values reported as the means with standard deviation

increased. At this temperature, the PAD purified in this study, lost 50% of activity within 38 min, a 65% loss after 4 h then little change thereafter.

Kinetic Analysis

A study into the effect of substrate concentration on the activity of PAD was investigated by measuring enzyme activity over a range of benzoyl arginine ethyl ester concentrations (0-4 mM). A typical increase in substrate concentration resulted in a proportional increase in activity until substrate saturation was achieved (Fig. 5). PAD activity of the enzyme purified in this study was rather low with a maximum activity (V_{max}) of 1.57 μmol min^{-1} ml^{-1} while a Michaelis constant (K_m) value of 1.35 mM

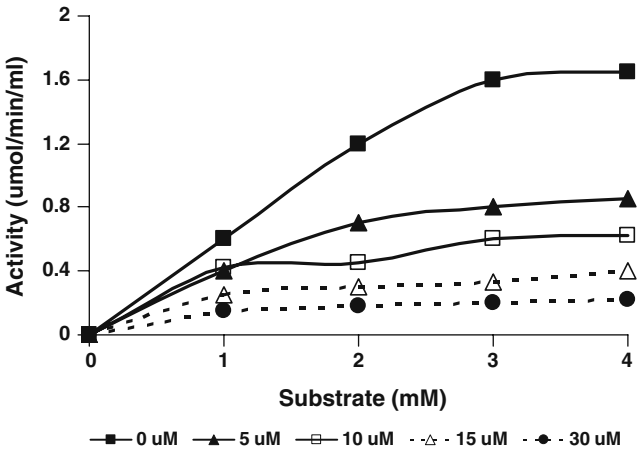

Fig. 5 Michaelis-Menten kinetic plot of PAD activity vs. benzoyl arginine ethyl ester substrate in the presence and absence of $A\beta_{1-40}$ amyloid peptides. Time for each incubation was 5 min. All analyses were carried in triplicate and values reported as the means with standard deviation

was recorded. Though there is considerable variation in the K_m values in the literature for PAD with this same substrate, a value of 1.36 mM has been reported [16].

Affinity of Amyloid Peptides for PAD

Kinetic Analysis

The affinity of PAD for various amyloid peptides was determined by including each peptide to a final concentration of 5, 10, 15 and 30 μM in the presence of the substrate benzoyl arginine ethyl ester (0-4 mM). The results indicated that with the inclusion of 5 μM $A\beta_{1\text{-}40}$ the V_{max} decreased considerably from 1.57 to 0.75 μmol $min^{-1}ml^{-1}$ (Fig. 5), while the K_m value remained unchanged at 1.35 mM; at 15 μM peptide the V_{max} decreased to 0.38 μmol $min^{-1}ml^{-1}$. With 5 and 15 μM $A\beta_{17\text{-}28}$ the V_{max} decreased to 0.55 and 0.36 μmol $min^{-1}ml^{-1}$, respectively (data not shown) while the K_m remained unchanged. The other peptides exhibited similar results (data not shown) indicating that all of the peptides interact and inhibit the enzyme to some degree. The respective affinity constants (K_i) were determined by the relationship (Eq. 2).

$$V_{max}^{app} = (V_{max} \times K_i)/(K_i + A\beta) \quad (2)$$

Where V_{max} and V_{max}^{app} are the maximal rate of the enzyme catalysed reaction in the absence and presence of a known concentration of amyloid peptide (Aβ). The affinity constants (Table 2) of the amyloid fragments were all reasonably similar indicating that the residues responsible for initial binding were between 17 and 35 with the strongest influence between residue 25 to 35. The fact that the K_m remained constant no matter what peptide fragment was used endorsed our understanding that they interacted with PAD at a site remote to the active site.

It was extremely interesting to note that with increasing incubation time of amyloid peptide ($A\beta_{1\text{-}40}$) with PAD there was a corresponding decrease in PAD activity up to 6 min (Fig. 6). Thereafter, there appeared to be a restoration of enzyme activity very close to its original value of 1.6 μmol $min^{-1}ml^{-1}$ followed by a second cycle of inhibition with a decrease in PAD activity over time. This cyclical phenomenon was repeated again until after approximately 20 min when enzyme activity had been fully restored and no further change was seen. This time-dependent observation suggested an association-dissociation between PAD and the amyloid peptide fragment of which the strength and time of effect was dependent on the type and concentration of the fragment. Furthermore, though it may be speculation, it pointed to the fact that PAD acted as a catalyst and converted the amyloid peptide into a form that was no longer capable of binding to the PAD. Initially, within a few hours of incubation, these forms of amyloid peptide were soluble fibrils that, as we will show later, undergo fibrillogenesis catalysed by PAD into insoluble fibrils. Since the PAD activity was restored to its original value after about 20 min, it ruled out any possibility that the fibrils blocked the enzyme active site.

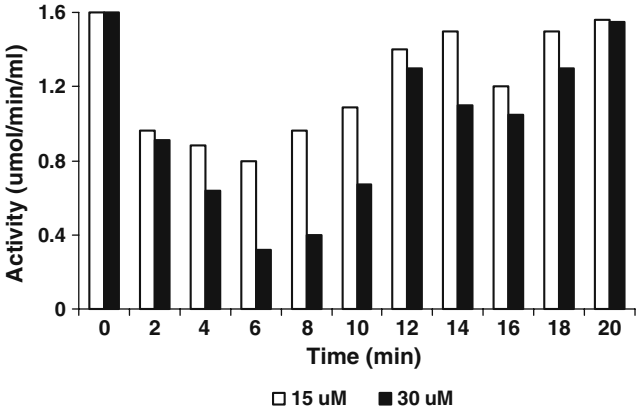

Fig. 6 Effect of $A\beta_{1\text{-}40}$ on PAD activity with respect to incubation time. Time zero=control reaction of initial enzyme activity without any inhibitor. All analyses were carried in triplicate and values reported as the means with standard deviation

Fibrillogenesis

The affinity of the amyloid peptides to PAD was also monitored by fluorescent staining with Thioflavin-T, Congo Red and turbidity assay in order to find the optimal conditions and kinetics for monitoring the PAD-induced Aβ aggregation and quantification of fibril formation. When each of the amyloid peptides ($A\beta_{1\text{-}40}$, $A\beta_{22\text{-}35}$, $A\beta_{17\text{-}28}$, $A\beta_{25\text{-}35}$, $A\beta_{32\text{-}35}$) at increasing concentrations was incubated with PAD in the presence of Thioflavin-T there was, with the exception of $A\beta_{32\text{-}35}$, a gradual increase in fluorescence up to a maximum at saturation (Fig. 7). This

Table 2 Affinity constants (K_i) and degree of fibrillogenesis (τ) measured by turbidity at 400 nm for the interaction of various amyloid peptide fragments with PAD

Peptide	Aβ (1-40)	Aβ (22-35)	Aβ (17-28)	Aβ (25-35)	Aβ (32-35)
K_i (μM)	4.6	3.04	2.7	1.4	2.9
τ	0.22	0.16	0.5	0.55	0.2

0.05 residual turbidity for PAD alone

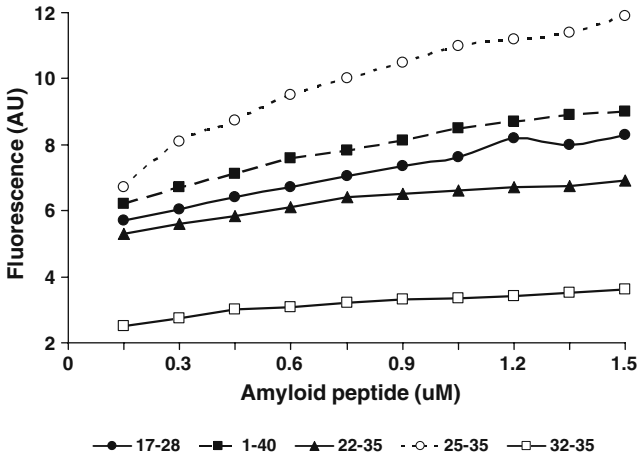

Fig. 7 PAD catalysed fibrillogenesis of amyloid peptide fragments ($A\beta_{1-40}$, $A\beta_{22-35}$, $A\beta_{17-28}$, $A\beta_{32-35}$ $A\beta_{25-35}$) quantified by Thioflavin-T fluorescence. All analyses were carried in triplicate and values reported as the means with standard deviation

change in fluorescence initially appeared to be linear, not only reflecting that PAD was indeed catalytic towards fibril formation, but indicated a direct estimation of both the concentration and rate of formation of fibrils. This was consistent with the possibility that the amyloid peptides were converted into a form that could no longer bind to the enzyme. PAD-induced $A\beta_{25-35}$ to produce fibrils both fourfold faster and more concentrated than those from $A\beta_{32-35}$ while the other peptides ($A\beta_{1-40}$, $A\beta_{22-35}$, $A\beta_{17-28}$) afforded rates of formation and concentrations only two- to threefold more.

In order to further investigate the effect of PAD as a catalyst for fibrillogenesis the Aβ peptides ($A\beta_{1-40}$, $A\beta_{22-35}$, $A\beta_{17-28}$, $A\beta_{32-35}$, $A\beta_{25-35}$) were incubated for several days at room temperature and amyloid fibril formation quantified by measuring the turbidity (τ) of the solution at 400 nm (Fig. 8). When no PAD enzyme was present, there was little or no formation of fibrils even after 168 h. It must be assumed that since no insoluble fibrils were formed in the absence of PAD, then no soluble fibrils would have been formed initially. A co-incubation with the enzyme, however, gave a clear indication of fibril formation after a time-lag phase of 24 h then exponentially increasing up to 168 h. The most prominent peptide fragments to undergo fibrillogenesis were the $A\beta_{17-28}$ and $A\beta_{25-35}$ with a ten- to 11-fold degree of fibril formation and $A\beta_{1-40}$ (fourfold; Fig. 8; Table 2). Peptides $A\beta_{32-35}$ and $A\beta_{22-35}$ gave between three- and fourfold degree of fibril formation (data not shown).

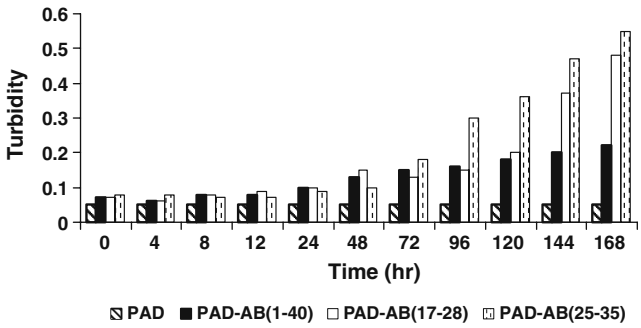

Fig. 8 Effect of $A\beta_{1-40}$, $A\beta_{17-28}$ and $A\beta_{25-35}$ on fibril formation as measured by the turbidity at 400 nm. All analyses were carried in triplicate and values reported as the means with standard deviation

The incubation of PAD, amyloid peptides and Thioflavin-T was only for 10 min ("Thioflavin-T Assay") and indicated that the formation of fibrils had occurred within several minutes. The turbidity assay, however, pointed to insoluble fibrils being formed only after 24-48 h (Fig. 8). This indicated that the fibrils that formed initially remained soluble and only with time did they aggregate sufficiently to precipitate from solution.

Finally, a Congo Red assay was performed to confirm the formation of the amyloid fibrils. Once again, it was noted that up to 24 h, the amyloid fibrils generated by the action of PAD on $A\beta_{1-40}$, $A\beta_{17-28}$ and $A\beta_{25-35}$ remained highly soluble with only slight turbidity seen (Fig. 9). After 24 h there was a rapid increase in the production of fibrils which, with the exception of $A\beta_{1-40}$ then gradually decreased with incubation time of 48–168 h. These data indicated that the fibrils that were formed from $A\beta_{17-28}$ and $A\beta_{25-35}$ became more and more insoluble with incubation time; fibrils from $A\beta_{1-40}$, however, remained in solution throughout. In the case of the $A\beta_{22-35}$ and $A\beta_{32-35}$, there was an insignificant amount of soluble fibrils formed up to 24 h incubation, thereafter only negative values were noted indicating, from Eq. 1, the presence of Congo Red alone and the complete precipitation of the fibrils.

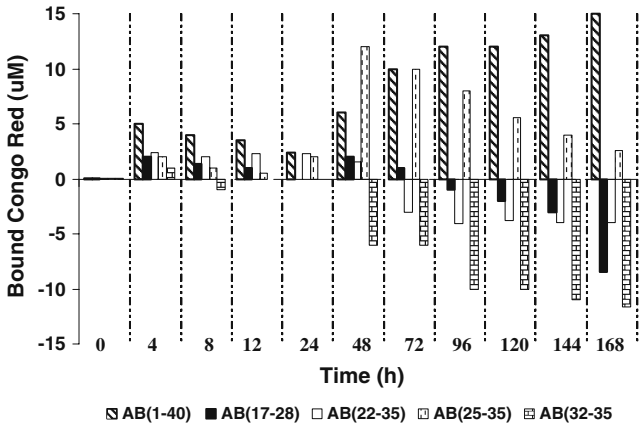

Fig. 9 Fibril formation, measured by Congo Red binding, after incubation of PAD with amyloid peptides (15 μM) at varying intervals up to 168 h. All analyses were carried in triplicate and values reported as the means with standard deviation

From the data obtained by both Thioflavin-T staining fluorescence and Congo Red assay, we were confident that the aggregates formed were in fact amyloid.

It has been documented in the literature that Aβ peptides interact with hydrophobic environments [21, 22] and so it was more than likely that PAD-Aβ complexes were hydrophobic-hydrophobic associations. Examining the amino acid sequence of the Aβ peptides that were readily induced to form fibrils pointed us towards two hydrophobic pentapeptide patches with sequences Leu $_{17}$–Val$_{18}$–Phe$_{19}$–Phe$_{20}$–Ala$_{21}$ and Gly$_{29}$–Ala$_{30}$–le$_{31}$–Ile$_{32}$–Gly $_{33}$. This latter sequence looked especially promising in view of the G-X-X-X-G protein/protein recognition motif [23]. We were very aware of a third hydrophobic pentapeptide G-X-X-X-G motif that existed with a sequence Gly$_{33}$–Leu$_{34}$–Met$_{35}$–Val$_{36}$–Gly$_{37}$. These characteristic glycine zipper motifs have been identified in many proteins as a transmembrane helix-turn-helix and, in the case of Aβ, were completely conserved suggesting that such motifs played an important role in their normal function. The fact that these peptides contain glycine zipper motifs has suggested that in vitro channel formation by these peptides could have serious implications in the aetiology and pathophysiology for Alzheimer's disease [24, 25]. In view of our present results, it was tempting to suggest that the hydrophobic patches and/or glycine zippers between residues 17 and 35 mediates, the process of fibrillogenesis of the amyloid peptides. To our knowledge, these peptides Gly$_{33}$–Leu$_{34}$–Met$_{35}$–Val$_{36}$–Gly$_{37}$ and Gly$_{29}$–Ala$_{30}$–Ile$_{31}$–Ile$_{32}$–Gly$_{33}$-Leu$_{34}$–Met$_{35}$–Val$_{36}$–Gly $_{37}$ were not commercially available and so their specific interaction with PAD was not investigated. They are being synthesised and will be the subject of a future study.

There is evidence [26–28] that fibrillogenesis of amyloid peptides may be catalysed by several biomacromolecules including enzymes and/or proteins. The actual specific mechanism remains elusive. By correlating the kinetic analysis, the Thioflavin-T fluorescence data and the Congo Red assay and turbidity assays for the affinity of several amyloid peptides with PAD, there was evidence to support a two-stage transition. Though we have no definitive proof whether the original peptide fragments were random coils or α-helices, there was evidence of a rapid conversion of the peptide, initiated by the enzyme, into a soluble β-conformation rendering it no longer able to bind with the

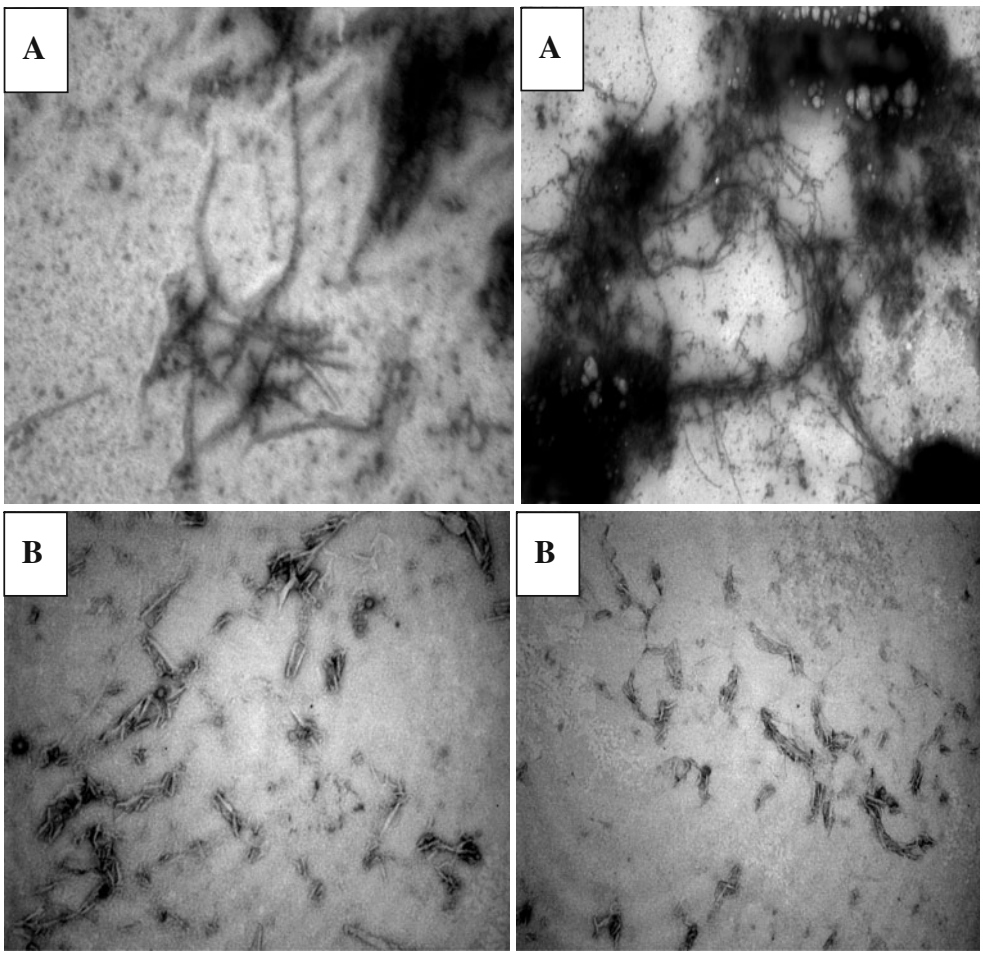

Fig. 10 Transmission electron microscopy views of **a** peptide Aβ$_{17-28}$ after incubation with PAD showing fibrils. **b** Peptide Aβ$_{17-28}$ alone

enzyme. Then after approximately 24 h, there was a further change, also initiated by PAD, and the formation of insoluble fibril aggregates.

Transmission Electron Microscopy

The structure of the insoluble amyloid fibrils generated from the proteolytic action of PAD with $A\beta_{17\text{-}28}$ was examined under transmission electron microscopy. They revealed extensive formation of fibrils (Fig. 10a) compared to the amyloid peptide before induction with PAD (Fig. 10b)

Concluding Comments

Amyloid peptides not only became bound to PAD but underwent catalytic fibrillogenesis by the enzyme. PAD was purified 137-fold in 12.5% yield on DEAE Sephacel with specific activity of 59 μmol min^{-1} mg $protein^{-1}$. It had a pH and temperature optima of 7.5 and 68°C, respectively, and was relatively stable under these conditions losing 50% of its activity within 38 min at this temperature. Kinetic analysis afforded a V_{max} of 1.6 μmol $min^{-1}ml^{-1}$ and a Michaelis constant (K_m) of 1.35 mM. Interaction of the various amyloid peptide fragments with PAD showed an association-dissociation suggesting that the enzyme acted as catalyst and converted the peptide into a form which could no longer bind. Determination of affinity constants revealed that $A\beta_{25\text{-}35}$ had, initially, the strongest affinity (K_i=1.4 μM) while the other peptide fragments had K_i values between 2 and 3 μM. Thioflavin-T staining fluorescence, Congo Red assay and turbidity assays at 400 nm indicated that $A\beta_{17\text{-}28}$ and $A\beta_{25\text{-}35}$ were the most prominent for fibrillogenesis and the rapid formation of soluble fibrils, that eventually, after 24 h, formed insoluble aggregates.

Finally, in support of our findings, we are confident that the hydrophobic pentapeptide patches and/or glycine zipper motifs between residues 17 and 37 were responsible for both initial binding and proteolytic catalysis into fibrils.

Acknowledgements The financial assistance from The Medical Research Council (South Africa) towards this research is hereby acknowledged.

References

1. Soto C, Branes MC, Alvarez J, Inestrosa NC (1994) Structural determinants of the Alzheimer's amyloid β-peptide. J Neurochem 63:1191–1198
2. Findeis MA (2007) The role of amyloid β-peptide 42 in Alzheimer's disease. Pharmacol Ther 116:266–286
3. Crouch PJ, Harding S-ME, White AR, Camakaris J, Bush AI, Masters CL (2008) Mechanisms of Aβ-mediated neurodegeneration in Alzheimer's disease. Int J Biochem Cell Biol 40:11648–11655
4. Guerrin M, Ishigami A, Mechin M-C, Nachat R, Valmary S, Sebbag M, Simon M, Senshu T, Serre G (2003) c DNA cloning, gene organisation and expression analysis of human peptidylarginine deiminase. Biochem J 370:167–174
5. Louw CA, Gordon A, Johnston N, Mollatt C, Bradley G, Whiteley CG (2007) Arginine deiminases: therapeutic tools in the etiology and pathogenesis of Alzheimer's disease. J Enzyme Inhib Med Chem 22(1):121–126
6. Iwata N, Tsubuki S, Takaki Y, Watanabe K, Sekiguchi M, Hosoki E, Kawashima-Morishima M, Lee HJ, Hama E, Sekine-Aizawa Y, Saido TC (2000) Identification of the major $A\beta_{1\text{-}42}$ degrading catabolic pathway in brain parenchyma:suppression leads to biochemical and pathological deposition. Nature (Medicine) 6:143–150
7. Gorevic PD, Castano EM, Sarma R, Frangione B (1987) Ten to fourteen residue peptides of Alzheimer's disease protein are sufficient for amyloid fibril formation and its characteristic X-ray diffraction pattern. Biochem Biophys Res Commun 147:854–862
8. Pike CJ, Walencewicz-Wasserman AJ, Kosmoski J, Cribbs DH, Glabe CG, Cotman CW (1995) Structure activity analyses of β-amyloid peptides: contribution of the $A\beta_{25\text{-}35}$ region to aggregation and neurotoxicity. J Neurochem 64:253–265
9. Soto C, Castano E, Frangione B, Inestrosa NC (1995) The α-helical to β-strand transition in the N-terminal fragment of the amyloid β-peptide modulates amyloid formation. J Biol Chem 266:4025–4028
10. Liao Y-F, Hsieh H-C, Liu G-Y, Hung H-C (2005) A continuous spectro-photometric assay method for peptidylarginine deiminase type 4 activity. Anal Biochem 347:176–181
11. Bradford MM (1976) A rapid and sensitive method for the quantification of microgram quantities of protein utilizing the principle of protein dye binding. Anal Biochem 72:248–254
12. Klunk WE, Pettegrew JW, Abraham DJ (1989) Two simple methods for quantifying low affinity dye-substrate binding. J Histochem Cytochem 37:1293–1297
13. Naiki H, Higuchi K, Nakakuki K, Takeda T (1991) Kinetic analysis of amyloid fibril polymerisation in vitro. Lab Invest 65:104–110
14. Le Vine H (1993) Thioflavin T interaction with synthetic Alzheimer's disease β-amyloid peptides: detection of amyloid aggregation in solution. Prot Sci 2:404–410
15. Le Vine H (1999) Quantification of β-sheet amyloid fibril structures with Thioflavin-T. Methods Enzymol 309:274–284
16. Kearney PL, Bhatia M, Jones NG, Yuan L, Glascock MC, Catchings KL, Yamada M, Thompson PR (2005) Kinetic characterization of protein arginine deiminase 4: a transcriptional corepressor implicated in the onset and progression of rheumatoid arthritis. Biochemistry 44:10570–10582
17. Nakayama-Hamada M, Suzuki A, Kubota K, Takazawa T, Ohsaka M, Kawaida R, Ono M, Kasuya A, Furukawa H, Yamada R, Yamamoto K (2005) Comparison of enzymatic properties between hPADI2 and hPADI4. Biochem Biophys Res Commun 327:192–200
18. Lamensa KWE, Moscarello MA (1993) Deimination of human myelin basic protein by a peptidylarginine deiminase from bovine brain. J Neurochem 61:987–996
19. McGraw W, Potempa J, Farley D, Travis J (1999) Purification, characterization, and sequence analysis of a potential virulence factor from *Porphyromonas gingivalis*. Peptidylarginine deiminase. Infect Immun 67:3248–3256
20. Luo Y, Arita K, Bhatia M, Knuckley B, Lee YH, Stallcup MR, Sato M, Thompson PR (2006) Inhibitors and inactivators of

protein arginine deiminase 4: functional and structural characterization. Biochemistry 45:11727–11736
21. Choo-Smith LP, Garzon-Rodriguez W, Glabe CG, Surewicz WK (1997) Acceleration of amyloid fibril formation by specific binding of $A\beta_{1-40}$ peptide to ganglioside-containing membrane vescicles. J Biol Chem 272:22987–22990
22. McLaurin JA, Franklin T, Fraser PE, Chakrabarty A (1998) Structural transitions associated with the interaction of Alzheimer β-amyloid peptides with gangliosides. J Biol Chem 273:4506–4515
23. Kim S, Jeon T-J, Oberai A, Yang D, Schmidt JJ, Bowie JU (2005) Transmembrane glycine zippers: physiological and pathological roles in membrane proteins. Proc Natl Acad Sci 102:14278–14283
24. Munter LM, Voigt P, Harmeier A, Kaden D, Gottschalk KE, Weise C, Pipkorn R, Schaefer M, Langosch D, Multhaup G (2007) GxxxG motifs within the amyloid precursor protein transmembrane sequence are critical for the etiology of $A\beta_{1-42}$. EMBO J 26:1702–1712
25. Yazawa H, Yu Z-X, Takeda Y, Le Y, Wanghua G, Ferrans VJ, Oppenheim JJ, Li CCH, Wang J (2001) β Amyloid peptide ($A\beta_{42}$) is internalized via the G-protein-coupled receptor FPRL1 and forms fibrillar aggregates in macrophages. FASEB J 15:2454–2462
26. Wetzel R (1999) Characterisation of in vitro protein deposition. Methods Enzymol 309:189–476
27. Esler WP, Stimson ER, Mantyth PW, Maggio JE (1999) Deposition of soluble β-amyloid onto amyloid templates: with applications for identification of amyloid fibril extension inhibitors. Methods Enzymol 309:350–74
28. Terzi E, Hölzemann G, Seelig J (1997) Interaction of Alzheimer β-amyloid $peptide_{1-40}$ with lipid membranes. Biochemistry 36:14845–14852